Endocannabinoids mediate bidirectional striatal spike-timing dependent plasticity

Yihui Cui, Vincent Paille, Hao Xu, Stéphane Genet, Bruno Delord, Elodie Fino, Hugues Berry, Laurent Venance

Endocannabinoids mediate bidirectional striatal spike-timing dependent plasticity

Yihui CUI[1,2], Vincent PAILLE[1,2], Hao XU[1,2], Stéphane GENET[2,3], Bruno DELORD[2,3], Elodie FINO[1,2], Hugues BERRY[4,5#] and Laurent VENANCE[1,2#]

[1]Center for Interdisciplinary Research in Biology, College de France, INSERM U1050, CNRS UMR7241, Labex Memolife, Paris, France

[2]University Pierre et Marie Curie, ED 158, Paris, France

[3]Institute of Intelligent Systems and Robotics (ISIR), Paris, France

[4]INRIA, Villeurbanne, France

[5]University of Lyon, LIRIS UMR5205, Villeurbanne, France

[#]Correspondence: hugues.berry@inria.fr, laurent.venance@college-de-france.fr

Running title: Endocannabinoids mediate bidirectional striatal STDP

Key words: endocannabinoids, synaptic plasticity, basal ganglia

Total number of words in the paper: 5094

KEY POINTS SUMMARY

- Although learning can arise from few or even a single trial, synaptic plasticity is commonly assessed under prolonged activation. Here, we explored the existence of rapid responsiveness of synaptic plasticity at corticostriatal synapses in a major synaptic learning rule, the spike-timing-dependent plasticity.

- We found that spike-timing-dependent depression (tLTD) progressively disappears when decreasing the number of paired stimulations (below 50 pairings) whereas spike-timing-dependent potentiation (tLTP) displays a biphasic profile: tLTP is observed for 75-100 pairings, is absent for 25-50 pairings and reemerges for 5-10 pairings.

- This tLTP induced by low numbers (5-10) of pairings depends on endocannabinoid system, type-1 cannabinoid receptor and transient receptor potential vanilloid type-1 activation.

- Endocannabinoid-tLTP may represent a physiological mechanism operating in the rapid learning of new associative memories and behavioral rules characterizing the flexible behavior of mammals or during the initial stages of habit learning.

ABSTRACT

Synaptic plasticity, a main substrate for learning and memory, is commonly assessed with prolonged stimulations. Since learning can arise from few or even a single trial, synaptic strength is expected to adapt rapidly. However, it remained elusive whether synaptic plasticity occurs in response to limited event occurrences. To answer this question, we investigated if a low number of paired stimulations can induce plasticity in a major synaptic learning rule, the spike-timing dependent plasticity (STDP). It is known that 100 pairings induce bidirectional STDP, i.e. spike-timing-dependent potentiation (tLTP) and depression (tLTD) at most central synapses. In rodent striatum, we found that tLTD progressively disappears when decreasing the number of paired stimulations (below 50 pairings) whereas tLTP displays a biphasic profile: tLTP is observed for 75-100 pairings, absent for 25-50 pairings and reemerges for 5-10 pairings. This tLTP, induced by very few pairings (~5-10), depends on the endocannabinoid (eCB) system. This eCB-tLTP involves postsynaptic endocannabinoid synthesis, is homosynaptic and depends on type-1 cannabinoid receptor (CB1R) and transient receptor potential vanilloid type-1 (TRPV1) activation. eCB-tLTP occurs in both striatopallidal and striatonigral MSNs and is dopamine-dependent. Lastly, we show that eCB-LTP and eCB-LTD can be induced sequentially in the same neuron, depending on the cellular conditioning paradigm. Thus, while usually considered as simply depressing synaptic function, endocannabinoids constitute a versatile system underlying bidirectional plasticity. Our results reveal a novel form of synaptic plasticity, eCB-tLTP, which may underlie rapid learning capabilities characterizing behavioral flexibility.

ABBREVIATIONS

2-AG: 2-arachidonoylglycerol

AP: action potential

AM251: N-(piperidin-1-yl)-5-(4-iodophenyl)-1-(2,4-dichlorophenyl)-4-methyl-1H-pyrazole-3-carboxamide

AMG9810: (2*E*)-*N*-(2,3-Dihydro-1,4-benzodioxin-6-yl)-3-[4-(1,1-dimethylethyl)phenyl]-2-propenamide

CB_1R: type 1 cannabinoid receptor

D_1R: type-1 dopaminergic receptor

D_2R: type-2 dopaminergic receptor

DAGLα: diacylglycerol lipase-α

D-AP5: DL-2-amino-5-phosphono-pentanoic acid

eCB: endocannabinoid

EPSC: excitatory postsynaptic current

LTD: long-term depression

tLTD: spike-timing-dependent long-term depression

LTP: long-term potentiation

tLTP: spike-timing-dependent long-term potentiation

MCPG: (S)-α-Methyl-4-carboxyphenylglycine

mGluR: metabotropic glutamate receptors

MPEP: 2-Methyl-6-(phenylethynyl)pyridine hydrochloride

MSN: medium-sized spiny neuron

PLCβ: phospholipase Cβ

STDP: spike-timing dependent plasticity

THL: tetrahydrolipstatin

TRPV1: transient receptor potential vanilloid-type-1

VSCC: voltage-sensitive calcium channels

INTRODUCTION

Cardinal cognitive abilities can display rapid learning dynamics. Forming new associative memories and behavioral rules can be learned within a few (5-10) or even a single trial (Schultz et al., 2003; Pasupathy and Miller, 2005; Tse et al., 2007; Quilodran et al., 2008; Ito and Doya, 2009). In cortex and striatum, neurons that respond to behaviorally relevant events (cues, actions or rewards) fire very few spikes (one to a dozen) upon each trial (i.e. they typically discharge at a frequency of 5-25Hz during a 0.1-0.5s period) (Schultz et al., 2003; Pasupathy and Miller, 2005; Quilodran et al., 2008). This evidence suggests that the discharge of a small number (2-50) of spikes should be sufficient to induce synaptic plasticity, a substrate for learning and memory (Martin and Morris, 2002). However, typical cell conditioning experimental protocols for initiating long-term plasticity, such as high- or low-frequency stimulations, rely on the repetition of hundreds of pre- or postsynaptic spikes. Noticeable exceptions are reports showing the existence of single-shock LTD in visual cortex or single-burst LTP in hippocampus (Holthoff and al., 2004; Remy and Spruston, 2007). Besides these reports introducing the possibility of bidirectional plasticity induced by limited stimulation, the possible existence of rapid responsiveness of synaptic plasticity still needs to be extended to other synapses and cell conditioning protocol.

Here, we tested the hypothesis that a low number of spikes could lead to long-term synaptic plasticity. For this purpose, we chose spike-timing dependent plasticity (STDP) as a synaptic learning paradigm. Indeed, STDP (tLTP and tLTD) depends on the relative timing between pre- and postsynaptic spikes, and relies on much fewer events (around 100 paired stimulations) than the high- or low-frequency stimulation protocols (hundreds of stimulations) (Caporale and Dan, 2008; Sjöström et al., 2008; Feldman, 2012). We first investigated if limited occurrences of paired stimulations, from 2 to100 pre-post or post-pre pairings, could induce STDP at corticostriatal synapses. In the striatum, bidirectional STDP with NMDAR-

mediated tLTP and endocannabinoid(eCB)-mediated tLTD, has been previously reported and was induced with 100 paired stimulations (Fino et al., 2005; Shen et al., 2008; Pawlak and Kerr, 2008; Fino et al., 2010; Fino and Venance, 2010; Paillé et al., 2013). In the present study we report that these forms of plasticity disappear when the number of paired stimulations is decreased. However, a reliable and robust tLTP re-emerges for a low number (~5-10) of paired stimulations. We show that this tLTP is not NMDAR-dependent but eCB-mediated. This eCB-tLTP depends on the activation of type-1 cannabinoid receptor (CB1R) and transient receptor potential vanilloid type-1 (TRPV1). eCB-tLTP can be induced in both striatopallidal and striatonigral MSNs and is dopamine-dependent. Finally, we observe that eCB-tLTP and eCB-tLTD can be sequentially induced at the same synapse, thus demonstrating that eCBs serve as a generic signaling system able to encode for bidirectional plasticity. eCBs have emerged as a major signaling system in learning and memory because of their powerful influence on synaptic plasticity that has been associated with the depression of neuronal communication on short or long timescales (Kano et al., 2009; Katona and Freund, 2012; Castillo et al., 2012; Mathur and Lovinger, 2012; Melis et al., 2014). eCB-tLTP reported here shows that eCBs in fact support bidirectional plasticity. This new form of plasticity may underlie the quick reactivity necessary for adapting the response of the synaptic weight during rapid learning.

METHODS

Animals

All experiments were performed in accordance with local animal welfare committee (Center for Interdisciplinary Research in Biology and EU guidelines (directive 2010/63/EU). Every precaution was taken to minimize stress and the number of animals used in each series of experiments. Sprague-Dawley rats (Charles River, L'Arbresle, France) and C57BL/6 mice $CB_1R^{-/-}$ (ledent et al., 1999) and D_1-eGFP mice were used for brain slice electrophysiology. Animals were housed in standard 12 hours light/dark cycles and food and water were available *ad libitum*.

Brain slice preparation

Horizontal brain slices containing the somatosensory cortex and the corresponding corticostriatal projection field were prepared according to the methods previously published (Fino et al., 2005; Paillé et al., 2013). Corticostriatal connections (between somatosensory cortex layer 5 and dorsal striatum) are preserved in a horizontal plane. Briefly, horizontal brain slices with a thickness of 330 or 300µm were prepared, respectively, from rats (males and females, $P_{(17-25)}$) or mice (males and females $P_{(17-25)}$ and $P_{(60-90)}$) using a vibrating blade microtome (VT1200S, Leica Micosystems, Nussloch, Germany). Brains were sliced in a 95% CO2/5% O2-bubbled, ice-cold cutting solution containing (in mM) 125 NaCl, 2.5 KCl, 25 glucose, 25 $NaHCO_3$, 1.25 NaH_2PO_4, 2 $CaCl_2$, 1 $MgCl_2$, 1 pyruvic acid, and then transferred into the same solution at 34°C for one hour and then moved to room temperature.

Electrophysiology recordings

Patch-clamp recordings were performed as previously described (Fino et al., 2010; Paillé et al., 2013). Briefly, borosilicate glass pipettes of 4-6MΩ resistance contained for whole-cell

recordings (in mM): 105 K-gluconate, 30 KCl, 10 HEPES, 10 phosphocreatine, 4 ATP-Mg, 0.3 GTP-Na, 0.3 EGTA (adjusted to pH 7.35 with KOH). The composition of the extracellular solution was (mM): 125 NaCl, 2.5 KCl, 25 glucose, 25 $NaHCO_3$, 1.25 NaH_2PO_4, 2 $CaCl_2$, 1 $MgCl_2$, 10μM pyruvic acid bubbled with 95% O_2 and 5% CO_2. Signals were amplified using EPC10-2 amplifiers (HEKA Elektronik, Lambrecht, Germany). All recordings were performed at 34°C using a temperature control system (Bath-controller V, Luigs&Neumann, Ratingen, Germany) and slices were continuously superfused at 2-3 ml/min with the extracellular solution. Slices were visualized on an Olympus BX51WI microscope (Olympus, Rungis, France) using a 4x/0.13 objective for the placement of the stimulating electrode and a 40x/0.80 water-immersion objective for localizing cells for whole-cell recordings. Medium-sized spiny neurons (MSNs), the striatal output neurons, were distinguished from interneurons based on passive and active membrane properties (Fino et al., 2008). Series resistance was not compensated. Current-clamp recordings were filtered at 2.5 kHz and sampled at 5 kHz and voltage-clamp recordings were filtered at 5 kHz and sampled at 10 kHz using the Patchmaster v2x32 program (HEKA Elektronik).

Chemicals

Chemicals were bath-applied or injected only in the recorded postsynaptic neuron through the patch-clamp pipette. DL-2-amino-5-phosphono-pentanoic acid (D-AP5, 50 μM) (Tocris, Ellisville, MO, USA), 2-Methyl-6-(phenylethynyl)pyridine hydrochloride (MPEP hydrochloride, 10 μM) (Tocris), 5,11-Dihydro-11-[(4-methyl-1-piperazinyl)acetyl]-6H-pyrido[2,3-b][1,4]benzodiazepin-6-one dihydrochloride (pirenzepine dihydrochloride, 1 μM) (Sigma) were dissolved directly in the extracellular solution and bath applied. N-(piperidin-1-yl)-5-(4-iodophenyl)-1-(2,4-dichlorophenyl)-4-methyl-1H-pyrazole-3-carboxamide (AM251, 3 μM) (Tocris), picrotoxin (50 μM) (Sigma), 1,4-Dihydro-2,6-dimethyl-4-(3-nitrophenyl)-3,5-

pyridinedicarboxylic acid 2-methyloxyethyl 1-methylethyl ester (nimodipine, 1 μM) (Tocris) and (2*E*)-*N*-(2,3-Dihydro-1,4-benzodioxin-6-yl)-3-[4-(1,1-dimethylethyl)phenyl]-2-propenamide (AMG9810, 1μM) (Tocris), R(+)-7-Chloro-8-hydroxy-3-methyl-1-phenyl-2,3,4,5-tetrahydro-1H-3-benzazepine hydrochloride (SCH-23390, 4μM, Sigma) and (S-)-5-Aminosulfonyl-N-[(1-ethyl-2-pyrrolidinyl)methyl]-2-methoxybenzamide (sulpiride, 10μM, Tocris) were dissolved in ethanol and then added in the external solution at a final concentration of ethanol of 0.01-0.1%. BAPTA (1 mM) (Sigma) and GDP-ß-S (2mM) were dissolved directly into the intracellular solution and applied via the patch-clamp pipette. U73122 (5 μM) (Sigma) was dissolved in ethanol and then added in the intracellular solution at a final concentration of ethanol of 0.033%. Tetrahydrolipstatin (THL, 10 μM) (Sigma) was dissolved in DMSO and applied internally via the patch-clamp pipette at a final concentration of DMSO of 0.1%. (S)-α-Methyl-4-carboxyphenylglycine (MCPG, 500 μM) (Tocris) was dissolved in 1.1 eq. NaOH, and then added in the external solution. N-[2-(4-Chlorophenyl)ethyl]-1,3,4,5-tetrahydro-7,8-dihydroxy-2H-2-benzazepine-2-carbothioamide (capsazepine, 10 μM) (Tocris) and 2-arachidonoylglycerol (2-AG, 100 μM) (Tocris) were dissolved in DMSO and then added in the external solution at a final concentration of DMSO of 0.0025 and 0.1%, respectively.

Note that none of the bath-applied drugs had a significant effect on basal EPSC amplitudes (Table 1).

Spike-timing-dependent plasticity induction protocols

Electrical stimulations were performed with a bipolar electrode (Phymep, Paris, France) placed in the layer 5 of the somatosensory cortex (Fino et al., 2005; Fino et al., 2010). Electrical stimulations were monophasic at constant current (ISO-Flex stimulator, AMPI, Jerusalem, Israel). Currents were adjusted to evoke 50-200pA EPSCs. Repetitive control stimuli were applied at 0.1Hz. STDP protocols consisted in pairings of pre- and postsynaptic

stimulations (at 1Hz) with the two events separated by a specific temporal interval (Δt_{STDP}). Presynaptic stimulations corresponded to cortical stimulations and the postsynaptic stimulation of an action potential evoked by a depolarizing current step (30ms duration) in MSNs. We chose to evoke a 30ms suprathreshold depolarization to mimic corticostriatal summation of EPSPs induced by cortical activity as observed in *in vivo* studies (Mahon et al., 2006). MSNs were maintained all along the STDP experiments at a constant holding membrane potential which corresponds to their initial resting membrane potential (-75±1 mV, n=103). Thus, EPSCs during baseline or after STDP protocol were mesured at the same membrane potential (in voltage-clamp mode); note that the STDP pairings (performed in current-clamp mode) were conducted also at this very same holding membrane potential. Neurons were recorded for 10 min during baseline and for at least 60 min after STDP protocol; long-term synaptic efficacy changes were measured from 50 min. 30 successive EPSCs were individually measured and then averaged. Variation of series resistance above 20% led to the rejection of the experiment. After recording of 10 min control baseline, drugs were applied in the bath. A new baseline with drugs was recorded after a time lapse of 10 min (to allow the drug to be fully perfused) for 10 min before STDP protocol (see effects of the bath-applied drugs on baseline in Table 1). Drugs were present until the end of the recording (except when specified). In a subset of experiments (for U73122, THL, BAPTA and GDP-ß-S) drugs were applied intracellularly through the patch-clamp pipette. Once the cell patched, drugs were allowed to diffuse into the cell during at least 15 minutes before starting the baseline recording. Local applications of 2-AG were performed through a patch-clamp pipette placed at the vicinity (50µm) of the recorded neuron and linked to a Picospritzer II system (Parker, USA), which supplies repeatable pressure pulses.

It should be noted that STDP protocol consisting in 5-10 post-pre pairings (with a single postsynaptic spike) were sufficient to induce potent tLTP in rat while in C57BL/6 mice 15 pairings (with 2-3 postsynaptic spikes) were necessary to trigger tLTP.

Electrophysiological data analysis

Off-line analysis was performed using Fitmaster (Heka Elektronik) and Igor-Pro 6.0.3 (Wavemetrics, Lake Oswego, OR, USA). Statistical analysis was performed using Prism 5.0 software (San Diego, CA, USA). In all cases "n" refers to a single cell experiment from single slice. Experimenters were blind to the genotype of $CB_1R^{-/-}$ and $CB_1R^{+/+}$ mice during electrophysiological recordings and analysis. All results were expressed as mean±s.e.m in the text and mean±s.d in the figures, and statistical significance was assessed using two-sided Student's t test or the one sample t test when appropriate at the significance level (p) indicated.

RESULTS

A low number of paired stimulations induces spike-timing dependent potentiation

We investigated if a low number of post- and presynaptic paired stimulations can induce plasticity in a major synaptic learning rule such as STDP. As previously described (Fino et al., 2005; Shen et al., 2008; Pawlak and Kerr, 2008; reviewed in Kreitzer and Malenka, 2008; Fino and Venance, 2010; Feldman, 2012), 100 pairings induced bidirectional STDP in MSNs: post-pre pairings ($-30<\Delta t_{STDP}<0$ ms) induced tLTP (mean value of the EPSC amplitude recorded 60 min after STDP protocol: 142±16%, p=0.0262, n=10), while pre-post pairings ($0<\Delta t_{STDP}<+30$ ms) induced tLTD (66±10%, p=0.0124, n=7) (Fig. 1A-C and 1I). We observed a similar bidirectional STDP with 75 pairings: post-pre and pre-post pairings induced tLTP (167±26%, p=0.0378, n=8) and tLTD (64±5%, p=0.0010, n=6), respectively (Fig. 1D and 1I). We then decreased the number of pairings to 50 and observed contrasting effects on synaptic plasticity: while a potent tLTD persisted with pre-post pairings (66±6%, p=0.0013, n=7), the tLTP usually associated with post-pre pairings disappeared (103±12%, p=0.7902, n=7) (Fig. 1E and 1I). In turn tLTD disappeared for 25 pre-post pairings (94±3%, p=0.0801, n=8) (Fig. 1F and 1I). On the post-pre side there was still no significant plasticity (132±24%, p=0.1985, n=11) following 25 pairings although half of the cells displayed tLTP and the other half no plasticity (Fig. 1F and 1I). Unexpectedly, decreasing the number of paired stimulations further to 10-5 pairings unveiled another trend: whereas 10 pre-post pairings failed to induce significant plasticity (99±10%, p=0.9267, n=9), 10 post-pre pairings were sufficient to induce a potent tLTP (165±11%, p<0.0001, n=27) (Fig. 1G and 1I). A similar picture was obtained even with 5 pairings: post-pre and pre-post pairings induced tLTP (139±13%, p=0.0087, n=16) and no significant plasticity (93±6%, p=0.2417, n=6), respectively (Fig. 1H-I). No significant plasticity was detected with 2 post-pre pairings (108±9%, p=0.4013, n=6) (Fig. 1I). In conclusion, tLTD disappears with decreasing the

number of paired stimulations whereas tLTP displays a biphasic profile since tLTP is observed for 75-100 pairings and 5-10 pairings (with similar amplitudes) and absent for 25-50 pairings.

10 pairings-tLTP is NMDAR-independent

We then questioned the mechanism of tLTD and tLTP induced by these different numbers of pairings. We observed that the corticostriatal 100 pairings-tLTD was CB_1R-dependent, as previously demonstrated (Shen et al., 2008; Pawlak and Kerr, 2008; Fino et al., 2010; Paillé et al., 2013). Indeed, pharmacological inhibition of CB_1R with AM251 (3μM) prevented the expression of 100 pairings-induced tLTD (106±6%, p=0.4153, n=5) (Fig. 2A). Note that AM251 alone (without electrical stimulation) had no effect on basal synaptic transmission (99±5%, p=0.7988, n=8) (Table 1), indicating that CB_1R had no constitutive activity at corticostriatal synapses. Similarly to the 100 pairings-tLTD, the 50 pairings-tLTD was prevented with AM251 (3μM) (114±17%, p=0.4541, n=7) (Fig. 2B). Thus, the pre-post corticostriatal tLTD was CB_1R-mediated.

Concerning the post-pre tLTP, we confirmed that the 100 pairings-tLTP was NMDAR-mediated since prevented with the selective NMDAR blocker D-AP5 (50μM) (104±5%, p=0.4310, n=5) (Fig. 2C), as previously reported (Shen et al., 2008; Pawlak and Kerr, 2008; Fino et al., 2010; Paillé et al., 2013). We then explored the mechanism of the tLTP induced by 10 post-pre pairings and found that it does not rely on the same signaling pathway (*i.e* NMDAR). Indeed, the tLTP induced by 10 pairings was not significantly affected by D-AP5 (169±22%, p=0.0098, n=13) (Fig. 2C), questioning the identity of the signaling pathways underlying this new form of tLTP.

10 pairings-tLTP involves postsynaptic 2-AG signaling

The corticostriatal synapse is glutamatergic and we first tested whether glutamatergic G-protein coupled receptors were required for the expression of tLTP induced by 10 pairings. MSNs express group-I metabotropic glutamate receptors (mGluRs) (Testa et al., 1994) belonging to the class of Gq/11-coupled receptors. 10 pairings-tLTP was prevented by the inhibition of group-I mGluR with MCPG (500μM) (100±8%, p=0.9636, n=5) (Fig. 3A-B). More specifically, among group-I mGluRs, MSNs express prominently the mGluR5 isoform (Uchigashima et al., 2007). MPEP (10μM), a blocker of mGluR5, prevented the induction of 10 pairings-tLTP and a slight depression was observed (68±8%, p=0.0108, n=6) (Fig. 3B). Besides glutamate, acetylcholine is also released following a cortical activation of the corticostriatal synapses: indirectly from striatal cholinergic interneurons (tonically active and directly contacted by cortical pyramidal cells). Interestingly, MSNs express the M1 muscarinic receptors that are also another class of Gq/11-coupled receptors (Hersch et al., 1994; Yamasaki et al., 2010). We thus tested if these receptors could be involved in the 10 pairings-tLTP. We found that the inhibition of M1 muscarinic receptors with pirenzepine (1μM) prevented tLTP (95±20%, p=0.8037, n=6) (Fig. 3B). Altogether, these results show that the tLTP triggered by 10 pairings requires the concomitant activation of mGluR5 and M1 muscarinic receptors. We investigated the postsynaptic localization of these receptors with the application in the recorded postsynaptic neuron of a non-hydrolysable nucleotide GDPβS that prevents G-protein activation (2mM i-GDPβS applied intracellularly through the patch-clamp pipette). i-GDPβS precluded tLTP (90±10%, p=0.3249, n=10) indicating that mGluR5 and M1 receptors were postsynaptically located (Fig. 3B). Group-I mGluRs and M1 receptors are Gq/11-coupled receptors and thus activate phospholipase Cβ (PLCβ) (Rebecchi and Pentyala, 2000). We then tested if PLCβ activation was involved in the 10 pairings-tLTP. In the presence of a PLCβ inhibitor applied intracellularly through the patch-clamp pipette (i-

U73122, 5μM) 10 post-pre pairings failed to induce any significant plasticity (94±7%, p=0.4255, n=5) (Fig. 3B), confirming the implication of postsynaptic PLCβ.

After activation by Gq/11-coupled receptors, PLCβ triggers large elevations in the concentration of calcium ions (Rebecchi and Pentyala, 2000). We therefore tested the involvement of calcium in the expression of 10 pairing-induced tLTP. We first showed that postsynaptic calcium elevation, in the recorded striatal neuron, was mandatory for tLTP induction. Indeed, specific loading of the recorded postsynaptic neuron with the fast calcium buffer BAPTA (10mM i-BAPTA applied intracellularly) prevented tLTP induction (108±10%, p=0.4774, n=5) (Fig. 3B). We next demonstrated that calcium entry via L-type voltage-sensitive calcium channels (VSCCs), the main type of activated VSCCs in MSNs (Carter and Sabatini, 2004), is responsible since their blockade (1μM nimodipine, 95±9%, p=0.6092, n=5) precluded tLTP (Fig. 3B). Further downstream in the signaling pathway, these concomitant activations are expected to promote diacylglycerol lipase-α (DAGLα) activity and therefore 2-arachidonoylglycerol (2-AG) synthesis (Hashimotodani et al., 2005; Piomelli et al., 2007; Di Marzo, 2008; Kano et al., 2009; Tanimura et al., 2010; Alger and Kim, 2011). 2-AG is produced from the PLCβ product diacylglycerol by calcium-activated DAGLα and is the principal eCB involved in modulating synaptic strength by selectively activating CB_1R (Piomelli et al., 2007). We found that DAGLα inhibitor, tetrahydrolipstatin (10μM i-THL applied intracellularly) prevented tLTP (91±7%, p=0.2607, n=5) (Fig. 3A-B). Importantly, since i-THL application was restricted to the recorded neuron, this result indicates that the production of 2-AG needed to activate CB_1R arises from the postsynaptic striatal neuron engaged in the paired stimulations. In summary, tLTP induced with 10 pairings involved the 2-AG synthesis pathway.

To further demonstrate the key role of 2-AG in bidirectional STDP (tLTD and tLTP with 100 pre-post pairings and 10 post-pre pairings, respectively), we applied local puffs of 2-AG of

different duration in the vicinity (50-100μm) of the recorded striatal neuron. We first applied 100 brief (300ms) puffs of 2-AG (100μM) at 1Hz, i.e the same total duration as a 100 pairings STDP protocol at 1Hz. In these conditions, we observed that without STDP protocol, 2-AG local application was able to induce a significant LTD (68±10%, p=0.0156, n=8) (Fig. 3C) with magnitude similar to the tLTD induced by 100 pre-post pairings (p=0.8624). This LTD involved CB_1R activation since 2-AG puffs did not induce plasticity anymore when AM251 (3μM) was bath-applied (96±5%, p=0.5000, n=6) (Fig. 3C).

We then aimed at mimicking the 10 pairing-induced LTP, by applying brief puffs of 2-AG (100μM) 10 times at 1Hz, thus with the same total duration as a 10 pairings STDP protocol at 1Hz. We observed that even in the absence of STDP protocol, 2-AG local application was able to induce a significant LTP (139±24%, p=0.0391, n=8) (Fig. 3D) with magnitude similar to the tLTP induced by 10 post-pre pairings (p=0.3705). This LTP involved CB_1R activation since 2-AG puff did not induce plasticity anymore in presence of AM251 (3μM) (92±4%, p=0.1542, n=5) (Fig. 3D).

10 pairings-tLTP is CB_1R activation mediated

Since 2-AG is a specific ligand of CB_1Rs (Piomelli et al., 2007; Di Marzo et al., 2008; Alger and Kim, 2011; Katona and Freund, 2012), we then asked whether tLTP induced by 10 pairings was indeed CB_1R-mediated. Pharmacological inhibition of CB_1R with AM251 (3μM) prevented the expression of 10 pairings-induced tLTP (80±11%, p=0.1424, n=6) (Fig. 4A).

This pharmacological result was further confirmed by experiments with CB_1R-knockout ($CB_1R^{-/-}$) mice (Ledent et al., 1999), where no significant plasticity was observed following 15 pairings (93±4%, p=0.0882, n=16) whereas tLTP could be induced in the wild-type $CB_1R^{+/+}$ mice (135±5%, p=0.0001, n=10) (Fig. 4B-C). Note that in C57BL/6 mice 15 pairings

with 2-3 APs were required to efficiently induced tLTP while 5-10 pairings with a single postsynaptic AP per pairing were sufficient to trigger tLTP in rats. This CB_1R-mediated tLTP was expressed up to adulthood since we observed a reliable tLTP in $P_{(60\text{-}90)}$ $CB_1R^{+/+}$ mice (137±8%, p=0.0109, n=5), which was absent in $P_{(60\text{-}90)}$ $CB_1R^{-/-}$ mice (93±6%, p=0.3048, n=5) (Fig. 4C). Pharmacological and genetic evidence demonstrated that tLTP induced by 10 pairings is eCB-mediated. We thus refer to this new form of LTP as eCB-tLTP.

eCB-LTP induction involves TRPV1

Besides 2-AG, the production of another eCB, anandamide, could also be increased upon cellular activity (Piomelli et al., 2007; Alger and Kim, 2011). Whereas 2-AG is a specific ligand of CB_1R, anandamide activates both CB_1R (albeit less potently than 2-AG) and TRPV1. TRPV1 is a nonselective cationic channel (Ross, 2003; Starowicz et al., 2007; Di Marzo, 2008) involved in eCB-mediated short- and long-term depression (Gibson et al., 2008; Maione et al., 2009; Chávez et al., 2010; Grueter et al., 2010; Puente et al., 2011). We therefore tested whether TRPV1 was implicated in eCB-tLTP. Note that in absence of paired stimulation, application of capsazepine (10μM), a TRPV1 antagonist, had no significant effect on basal EPSC (100±9%, p=0.9778, n=6) (Table 1), indicating that TRPV1 have no constitutive activity at corticostriatal synapses. We then found that the application of capsazepine (10μM) during the STDP stimulation protocol (10 post-pre pairings) blocked eCB-tLTP (83±11%, n=6, p=0.1133) (Fig. 5). To confirm this result, we used AMG9810, another competitive TRPV1 antagonist, structurally distinct from capsazepine, and observed that AMG9810 (1μM) also blocked eCB-tLTP (93±6%, p=0.3046, n=5) (Fig. 5B; Table 1).

Altogether, our results demonstrate that 10 pairings-tLTP is mediated by eCB (2-AG and anandamide), acting on both CB_1R and TRPV1.

eCB-tLTP occurs in both striatopallidal and striatonigral MSNs and is dopamine-dependent

Pyramidal cells from cortex layer 5 contact two MSN subpopulations belonging to the direct (striatonigral) or indirect (striato-pallido-subthalamo-nigral) trans-striatal pathways (Gerfen and Surmeier, 2011; Calabresi et al., 2014). We investigated wether eCB-tLTP are similarly induced in both striatopallidal and striatonigral MSNs. The two MNs subtypes express different dopaminergic receptors (D_1R-like and D_2R-like for the direct and indirect pathways, respectively) allowing us to identify them with transgenic D_1-eGFP mice and to investigate eCB-tLTP occurrence in D_1^+ and non-D_1^+ MSNs (Fig. 6A-B). We observed that 15 post-pre pairings (see Methods) induced tLTP in both D_1^+ (165±18%, p=0.0166, n=7) and non-D_1^+ (156±20%, p=0.0215, n=9) (Fig. 6A-B). This indicates that tLTP can be induced with few pairings in both striatopallidal and striatonigral MSNs.

Striatum receives excitatory afferents from the cortex as well as a dense innervation from midbrain dopaminergic neurons. Dopamine, a key regulator of action selection and associative learning (Yin and Knowlton, 2006; Redgrave and Gurney, 2006; Schultz, 2007), efficiently modulates corticostriatal synaptic plasticity and particularly the "classical" eCB-LTD (Kreitzer and Malenka, 2008; Di Filippo et al., 2009; Gerfen and Surmeier, 2011). We then asked whether dopamine was involved in eCB-tLTP induction. We examined which dopaminergic receptor subtype is involved in eCB-tLTP. For this purpose we first bath-applied a mixture of D_1R and D_2R antagonists, SCH23390 (4µM) and sulpiride (10µM), respectively. We found that this cocktail prevented the induction of eCB-tLTP and a depression was observed (75±2%, p<0.0001, n=7) (Fig. 6B). Thus, eCB-tLTP is dopamine-dependent. We then selectively inhibited either D_1R or D_2R. When we applied a D_1R antagonist, SCH23390 (4µM), we observed a potent tLTP (149±16%, p=0.0211, n=7) while tLTD could be elicited when a D_2R antagonist, sulpiride (10µM), was bath-applied (68±10%,

p=0.0209, n=7) (Fig. 6C). This indicates that eCB-tLTP is D_2R-mediated and not dependent on D_1R.

Corticostriatal eCB-tLTP is homosynaptic

To test the homosynaptic feature of eCB-tLTP we performed paired recordings of two neighboring MSNs (perisomatic distance<50µm) in which one neuron was subjected to 10 post-pre pairings (STDP protocol) while the second received only 10 presynaptic stimulations (n=6 pairs) (Fig. 6A). We observed a potent tLTP (150±13%, p=0.0143, n=6) only in the neuron subjected to post-pre pairings, while the neighboring neuron, that received only the presynaptic stimulation, did not show any significant plasticity (106±3%, p=0.0833, n=6) indicating that corticostriatal eCB-tLTP is homosynaptic.

In hippocampus, facilitation of LTP via eCB-induced presynaptic depression of GABAergic transmission has been reported (Carlson et al., 2002; Chevaleyre and Castillo, 2004; Zhu and lovinger, 2007). Here, the observed eCB-tLTP could arguably arise from a decrease of GABA release, through an activation of CB_1Rs located on GABA terminals, thus decreasing the inhibitory tonus during the pairing paradigm. To test this hypothesis, we blocked the $GABA_A$ receptors with picrotoxin (50µM). A significant tLTP was still observed for 10 pairings (135±12, n=6; p=0.0300) (Fig. 7B). The magnitude of 10 pairings-tLTP was not affected by a blockade of $GABA_A$ transmission since there was no significant difference with those observed in control condition (p=0.1200). As we recently described for STDP induced by 100 pairings (Paillé et al., 2013), GABA controls the polarity of the timing-dependance of STDP: with a blockade of $GABA_A$ transmission, tLTP was induced for 10 pre-post pairings (n=6) while post-pre pairings did not induce plasticity (96±7, p=0.5865, n=7) (Fig. 7B). We confirmed that this tLTP was eCB-mediated: the co-application of picrotoxine (50µM) and AM251 (3µM) prevented the induction of tLTP (103±7%, p=0.7454, n=5) (Fig. 7B). In

conclusion, GABAergic microcircuits are not involved in the synaptic efficacy changes themselves induced by 10 pairings but control the polarity of the timing-dependence of the eCB-tLTP.

Bidirectional eCB-STDP in the same neuron

eCB-tLTP and eCB-tLTD could represent functional inverses of each other. This could be demonstrated if both phenomena could be sequentially triggered in the same neuron to modify the synaptic weight and then bring it back to its baseline. We tested this hypothesis by applying successively two protocols leading to unidirectional plasticity, which exclusively imply eCBs: 10 post-pre pairings (eCB-tLTP) (Fig. 4) and 50 pre-post pairings (eCB-tLTD) (Fig. 2B). We found that eCB-tLTP and eCB-tLTD can indeed be induced sequentially in the very same neuron independently of the order of induction protocols (n=5) (Fig. 8). Following eCB-LTP induction by 10 post-pre pairings, the potentiated synaptic weight can be decreased back to its basal level by applying 50 pre-post pairings (Fig. 7A). Symmetrically, the synaptic weight depressed by an eCB-tLTD could be re-increased by eCB-tLTP induction in the same neuron (Fig. 8). These results demonstrate that eCB-tLTP and eCB-tLTD can be induced sequentially in the same neuron.

DISCUSSION

Corticostriatal long-term plasticity provides a fundamental mechanism for the function of the basal ganglia in action selection and in procedural learning (Yin and Knowlton, 2006; Yin et al., 2009; Koralek et al., 2012). Thus, characterizing striatal plasticity repertoire in physiological conditions is crucial. The striatum receives a wide range of patterns of cortical activities from isolated trains of few spikes to prolonged bursting events. While corticostriatal plasticity under prolonged activation is well elucidated, its occurrence to few spikes remained unexplored. Here, we uncovered the existence of an eCB-tLTP induced by a low number of pairings in the striatum of both juvenile and adult rodents. Indeed, few (5-10) coincident pre- and postsynaptic spikes were found to strengthen synaptic efficacy through a signaling pathway that relies on eCB system. eCB-tLTP induction relies on activation of CB_1R and TRPV1 and on 2-AG elevations triggered by coupled rises of calcium and DAGLα activity (mediated by mGluR5, muscarinic M1 receptors and VSCCs) in MSNs. Both activation of glutamatergic afferents from cerebral cortex and striatal cholinergic interneurons (which are monosynaptically contacted by cortical pyramidal cells (Fino et al., 2008)) promote the induction of eCB-tLTP.

We also found that eCB-tLTP is dopamine-dependent. More precisely, eCB-tLTP is D_2R-mediated and not dependent on D_1R. We then questioned the localization (pre- or postsynaptic) of the D_2R involved in eCB-tLTP. The postsynaptic localization at MSNs was *a priori* less likely. Indeed, due to the segregation of expression of D_1R and D_2R among MSNs (Kreitzer and Malenka, 2008; Gerfen and Surmeier, 2011; Calabresi et al., 2014), roughly half of MSNs are expected to be D_2R-expressing neurons. If eCB-tLTP was supported by the postsynaptic D_2R MSNs, one would expect to induce eCB-tLTP in ~50% of the (randomly chosen) neurons. In our experiments, eCB-tLTP was successfully induced in 83% of the (randomly chosen) tested MSNs in rats, thus suggesting a presynaptic localization of the D_2R.

Moreover, this was confirmed with experiments performed in D_1R-eGFP mice show that eCB-tLTP can be induced in both striatopallidal and striatonigral MSNs. This suggests that D_2Rs involved in eCB-tLTP are not postsynaptically located. Presynaptic D_2R are expressed at three different locations: the nigrostriatal dopaminergic afferents (De Mei et al., 2009), the cholinergic interneurons (Hersch et al., 1995) and the corticostriatal glutamatergic afferents (Bamford et al., 2004). The precise locus of presynaptic D_2R involved in eCB-tLTP remains to be determined.

We describe here a homosynaptic tLTP in mammals, wherein eCB signaling directly underlies both the induction and the long-term maintenance of synaptic weight increase. eCB signaling exhibits bidirectional plasticity with eCB-tLTP and eCB-tLTD. Bidirectionality is of paramount functional importance since it allows LTP and LTD to reverse each another at a single synapse.

eCBs have emerged as a major actor in learning and memory because of their powerful influence on synaptic plasticity (Katona and Freund, 2012; Castillo et al., 2012; Melis et al., 2014). The eCB system is mainly composed of biolipids synthesized and released on-demand acting as retrograde neurotransmitters on presynaptic CB_1R (one of the most abundant G protein-coupled receptors in the brain) and postsynaptic TRPV1. eCBs have been reported to depress synaptic weight, i.e. short- or long-term depression, through the activation of CB_1R (Kano et al., 2009; Katona and Freund, 2012; Castillo et al., 2012; Melis et al., 2014) or TRPV1 (Gibson et al., 2008; Maione et al., 2009; Chávez et al., 2010; Grueter et al., 2010; Puente et al., 2011). Noticeable exceptions are reports of an indirect role of eCBs in promoting LTP at mixed (chemical and electrical) synapses of the goldfish Mauthner cell *via* intermediary dopaminergic neurons (Cachope et al., 2007) or at hippocampal CA1 synapses via a $GABA_A$ receptor-mediated mechanism (Lin et al., 2011; Xu et al., 2012), facilitation of LTP in the hippocampus via eCB-induced presynaptic depression of GABAergic transmission

(Carlson et al., 2002; Chevaleyre and Castillo, 2004; Zhu and Lovinger, 2007), and mediation of heterosynaptic short-term potentiation *via* intermediary astrocytes (Navarrete and Araque, 2010). However, to our knowledge, the present study is the first report of a homosynaptic eCB-dependent LTP in mammals, with direct implication of eCBs in the induction and long-term maintenance of spike-timing-dependent potentiation of the stimulated synapse itself.

mGluR5 and M1R need to be simultaneously activated to elicit eCB-tLTP. Both receptors (mGluR5 and M1) are Gq/11-coupled receptors and positively coupled to PLCβ, thus leading to DAG production, and favoring the synthesis of 2-AG. Whereas cholinergic activation is not sufficient to trigger eCB-LTP, it remains necessary for the eCB-LTP induction. Our hypothesis is that eCB-LTP is induced only when large levels of 2-AG are produced. Our results of M1, mGluR5, VSCC and TRPV1 blocking indicate that it is mandatory to activate all possible cumulative contributions to 2-AG production (PLCβ activation for DAG production, VSCC and TRPV1 to increase calcium surge, thus activating DAGLα) in order to reach large levels of 2-AG, which would promote eCB-tLTP.

Just like in hippocampal pyramidal cells (Shouval et al., 2002; Graupner and Brunel, 2012), postsynaptic calcium levels (or time course) could be crucial in the induction of eCB-STDP in the striatum. Since many of the steps along the eCB pathways are Ca^{2+}-dependent (incl. 2-AG and anandamide synthesis), the "Ca^{2+} hypothesis" would translate to the CB_1R pathway. This would lead to a scenario where low to moderate peak levels of eCB would lead to LTD whereas high eCB levels would yield LTP. According to this scenario, our results could be reconciled if the first 5-20 post-pre pairings produce very large peak levels of 2-AG, thus tLTP. If the amplitude of the 2-AG peaks decreases for subsequent post-pre pairings, this initial tLTP would be de-potentiated by the subsequent pairings, thus restricting the expression of eCB-tLTP to the first 5 to 20 pairings. On the other hand, the LTP observed with 100 post-pre pairings entirely results from an increase of the postsynaptic weight through

activation of the CaMKII pathway by NMDARs, with no additional contribution of the eCB-LTP; indeed, when CB_1R was inhibited, the NMDAR-tLTP induced with 100 post-pre pairings was not significantly affected (Fino et al., 2010). Thus, eCB-LTP would start to be expressed after 5-20 post-pre pairings. Subsequent pairings would then erase this potentiation while, independently, triggering the expression of NMDA-LTP.

There is a large diversity of the STDP rules at play in the brain and even within the same structure, variety seems to be the rule (Feldman, 2012). Indeed, in striatum the main neuronal population, the MSNs, express NMDAR-tLTP and eCB-tLTD (Shen et al., 2008; Pawlak and Kerr, 2008; Fino et al., 2010; Paillé et al., 2013) and eCB-tLTP (the present report). Whereas neighbouring striatal fast-spiking GABAergic interneurons express solely NMDAR-dependent STDP, both for LTP and LTD, for 100 pairings (Fino et al., 2008) but lack plasticity at low numbers of pairings (data not shown). In addition, our results evidence that eCB-tLTP is anti-Hebbian at corticostriatal synapses and tightly controlled by GABAergic interneurons similarly to the bidirectional corticostriatal STDP (i.e. NMDAR-tLTP and eCB-tLTD; Paillé et al., 2013). It has been reported that the endocannabinoid-mediated LTP at hippocampal CA1 synapses induced with high-frequency (Lin et al., 2011), low-frequency (Zhu and Lovinger, 2007) or paired stimulations (Xu et al., 2012) were prevented not only by inhibition of CB_1R but also by inhibition of $GABA_A$ receptors. Here, we show that GABA is not involved in eCB-tLTP induction or magnitude at corticostriatal synapses but controls the polarity of eCB-tLTP.

Due to their on-demand intercellular signaling *modus operandi* (Alger and Kim, 2011) eCB biosynthesis and release are evoked by precisely timed and positioned physiological stimuli (Katona and Freund, 2008). As previously described, our study confirms that STDP indeed efficiently triggers eCB signaling. Evidence for TRPV1 activation by physiological neuronal activity patterns was lacking. We demonstrate here that STDP is able to engage the TRPV1

signaling pathway. TRPV1 being a cationic channel highly permeable to calcium (Ross, 2003; Starowicz et al., 2007; Di Marzo, 2008) it may contribute to eCB-tLTP induction by boosting the calcium transients in the postsynaptic element. As recently described for short- and long-term depression (Puente et al., 2011), our results illustrate the versatility of eCB signaling as a system displaying polymodal activation through CB_1R and TRPV1, to trigger LTP.

eCB-LTP is promoted by very low numbers of pairings (~5-10), therefore providing a mechanism whereby synapses react to the very first occurrences of incoming activity. This ability contrasts strongly with NMDAR-dependent LTP that requires the iteration of at least 75-100 paired stimulations to be expressed in the classical (1Hz) STDP context. In mammals, associative memories and behavioral rules can be learned within few (5-10) trials or even sometimes within a single trial (Pasupathy and Miller, 2005; Tse et al., 2007; Schultz et al., 2003; Quilodran et al., 2008; Ito and Doya, 2009). In cortex or striatum, neurons with behavior-related activities fire a few spikes upon behaviorally relevant events during each trial (i.e. at frequency 5-25Hz and during 0.1-0.5s, typically <10 spikes) (Pasupathy and Miller, 2005; Schultz et al., 2003; Quilodran et al., 2008), suggesting that a few trials should be sufficient to induce synaptic plasticity. eCB-tLTP may be used for learning and memorizing salient events from a few spikes. Hence, eCB-LTP may represent a molecular substrate operating in rapid learnings of new arbitrary associative memories and behavioral rules characterizing the flexible behavior of mammals or during initial stages of slower habit learnings (Barnes et al., 2011). Moreover, marijuana intoxication leads to impairment of working memory. This impairment was hitherto interpreted solely as the effect of cannabinoids on the promotion of synaptic depression. Our results together with recent reports (Lin et al., 2011; Xu et al., 2012) open new perspectives since they suggest that synaptic potentiation may as well be implied in the effects of marijuana.

Reference

Alger BE & Kim J (2011). Supply and demand for endocannabinoids. *Trends Neurosci* **34**, 304-315.

Bamford NS, Robinson S, Palmiter RD, Joyce JA, Moore C & Meshul CK (2004). Dopamine modulates release from corticostriatal terminals. *J. Neurosci.* **24,** 9541–9552.

Barnes TD, Mao JB, Hu D, Kubota Y, Dreyer AA, Stamoulis C, Brown EN & Graybiel AM (2011). Advance cueing produces enhanced action-boundary patterns of spike activity in the sensorimotor striatum. *J Neurophysiol* **105**, 1861-1878.

Cachope R, Mackie K, Triller A, O'Brien J & Pereda AE (2007). Potentiation of electrical and chemical synaptic transmission mediated by endocannabinoids. *Neuron* **56**, 1034-1047.

Calabresi P, Picconi B, Tozzi A, Ghiglieri V & Di Filippo (2014) Direct and indirect pathways of basal ganglia: a critical reappraisal. *Nat Neurosci* **17**, 1022-1030.

Caporale N & Dan Y (2008). Spike timing-dependent plasticity: a Hebbian learning rule. *Annu Rev Neurosci* **31**, 25-46.

Carlson G, Wang Y & Alger BE (2002). Endocannabinoids facilitate the induction of LTP in the hippocampus. *Nat Neurosci* **5**, 723-724.

Carter AG & Sabatini BL (2004). State-dependent calcium signaling in dendritic spines of striatal spiny neurons. *Neuron* **44**, 483-493.

Castillo PE, Younts TJ, Chavez AE & Hashimotodani Y (2012). Endocannabinoid signaling and synaptic function. *Neuron* **76**, 70-81.

Chávez AE, Chiu CQ & Castillo PE (2010). TRPV1 activation by endogenous anandamide triggers postsynaptic long-term depression in dentate gyrus. *Nat Neurosci* **13**, 1511-1518.

Chevaleyre V & Castillo PE (2004). Endocannabinoid-mediated metaplasticity in the hippocampus. *Neuron* **43**, 871-881.

De Mei C, Ramos M, Iitaka C & Borrelli E (2009). Getting specialized: presynaptic and postsynaptic dopamine D2 receptors. *Curr. Opin. Pharmacol.* **9,** 53–58.

Di Filippo M, Picconi B, Tantucci M, Ghiglieri V, Bagetta V, Sgobio C, Tozzi A, Parnetti L & Calabresi P (2009). Short-term and long-term plasticity at corticostriatal synapses: Implications for learning and memory. *Behav Brain Res* **199,** 108–118.

Di Marzo V (2008). Endocannabinoids: synthesis and degradation. *Rev Physiol Biochem Pharmacol* **60**, 1-24.

Feldman DE (2012). The spike-timing dependence of plasticity. *Neuron* **75**, 556-571.

Fino E, Glowinski J & Venance L (2005). Bidirectional activity-dependent plasticity at corticostriatal synapses. *J Neurosci* **25**, 11279-11287.

Fino E, Deniau JM & Venance L (2008). Cell-specific spike-timing-dependent plasticity in GABAergic and cholinergic interneurons in corticostriatal rat brain slices. *J Physiol* **586**, 265-282.

Fino E, Paille V, Cui Y, Morera-Herreras T, Deniau JM & Venance L (2010). Distinct coincidence detectors govern the corticostriatal spike timing-dependent plasticity. *J Physiol* **588**, 3045-3062.

Fino E & Venance L (2010). Spike-timing dependent plasticity in the striatum. *Front Synaptic Neurosci* **2**, 6.

Gerfen CR & Surmeier DJ (2011) Modulation of striatal projection systems by dopamine. *Annu Rev Neurosci* **34**, 441–466.

Gibson HE, Edwards JG, Page RS, Van Hook MJ & Kauer JA (2008). TRPV1 channels mediate long-term depression at synapses on hippocampal interneurons. *Neuron* **57**, 746-759.

Graupner M & Brunel N (2012). Calcium-based plasticity model explains sensitivity of synaptic changes to spike pattern, rate, and dendritic location. *Proc. Natl. Acad. Sci.* **109,** 3991–3996.

Grueter BA, Brasnjo G & Malenka RC (2010). Postsynaptic TRPV1 triggers cell type-specific long-term depression in the nucleus accumbens. *Nat Neurosci* **13**, 1519-1525.

Hashimotodani Y, Ohno-Shosaku T, Tsubokawa H, Ogata H, Emoto K, Maejima T, Araishi Shin H-S & Kano M (2005). Phospholipase Cβ serves as a coincidence detector through its Ca2+ dependency for triggering retrograde endocannabinoid signal. *Neuron* **45**, 257-268.

Hersch SM, Gutekunst C, Rees HD, Heilman CJ & Levey AI (1994). Distribution of m1-m4 muscarinic receptor proteins in the rat striatum: light and electron microscopic immunocytochemistry using subtype-specific antibodies. *J Neurosci* **17**, 3334-3342.

Hersch SM, Ciliax BJ, Gutekunst CA, Rees HD, Heilman CJ, Yung KK, Bolam JP, Ince E, Yi H & Levey AI. (1995). Electron microscopic analysis of D1 and D2 dopamine receptor proteins in the dorsal striatum and their synaptic relationships with motor corticostriatal afferents. *J. Neurosci.* **15,** 5222–5237.

Holthoff K, Kovalchuk Y, Yuste R & Konnerth A (2004). Single-shock LTD by local dendritic spikes in pyramidal neurons of mouse visual cortex. *J Physiol* **560**, 27-36.

Ito M & Doya K (2009). Validation of decision-making models and analysis of decision variables in the rat basal ganglia. *J Neurosci* **29**, 9861-9874.

Kano M, Ohno-Shosahu T, Hashimotodani Y, Uchigashima M & Watanabe M (2009). Endocannabinoid-mediated control of synaptic transmission. *Physiol Rev* **89**, 309-380.

Koralek, A. C., Jin, X., Long, J. D., Costa, R. M., and Carmena, J. M. (2012). Corticostriatal plasticity is necessary for learning intentional neuroprosthetic skills. Nature *483*, 331-335.

Katona I & Freund TF (2008). Endocannabinoid signaling as a synaptic circuit breaker in neurological disease. *Nat Med* **14**, 923-930.

Katona I & Freund TF (2012). Multiple functions of endocannabinoid signaling in the brain. *Annu Rev Neurosci* **35**, 529-558.

Kreitzer AC & Malenka RC (2008) Striatal Plasticity and Basal Ganglia Circuit Function. *Neuron* **60**, 543–554.

Ledent, C. Valverde O, Cossu G, Petitet F, Aubert JF, Beslot F, Böhme GA, Imperato A, Pedrazzini T, Roques BP, Vassart G, Fratta W & Parmentier M (1999). Unresponsiveness to cannabinoids and reduced addictive effects of opiates in CB1 receptor knockout mice. *Science* **283**, 401–404.

Lin QS, Yang Q, Liu DD, Sun Z, Dang H, Liang J, Wang YX, Chen J & Li ST (2011). Hippocampal endocannabinoids play an important role in induction of long-term potentiation and regulation of contextual fear memory formation. *Brain Res Bull* **86**, 139-145.

Mahon S, vautrelle N, Pezard L, Slaght SJ, Deniau JM, Chouvet G & Charpier S (2006). Distinct patterns of striatal medium spiny neuron activity during the natural sleep-wake cycle. *J Neurosci* **26**, 12587-12595.

Maione S, Cristino L, Migliozzi AL, Georgiou AL, Starowicz K, Salt TE & Di Marzo V (2009). TRPV1 channels control synaptic plasticity in the developing superior colliculus. *J Physiol* **587**, 2521-2535.

Mathur BN & Lovinger DM (2012). Endocannabinoid-dopamine interactions in striatal synaptic plasticity. *Frontiers Pharmacol* **3**, 1-11.

Martin SJ & Morris RG (2002). New life in an old idea: the synaptic plasticity and memory hypothesis revisited. *Hippocampus* **12**, 609-636.

Melis M, Greco B & Tonini R (2014). Interplay between synaptic endocannabinoid signaling and metaplasticity in neuronal circuit function and dysfunction. *Eur J Neurosci* **39**, 1189-1201.

Navarrete M & Araque A (2010). Endocannabinoids potentiate synaptic transmission through stimulation of astrocytes. *Neuron* **68**, 113-126.

Pasupathy A & Miller EK (2005). Different time courses of learning-related activity in the prefrontal cortex and striatum. *Nature* **433**, 873-876.

Paillé V, Fino E, Du K, Morera Herreras T, Perez S, Hellgren Kotaleski J & Venance L (2013). GABAergic circuits control spike-timing-dependent plasticity. *J Neurosci* **33**, 9353-9363.

Pawlak V & Kerr JN (2008). Dopamine receptor activation is required for corticostriatal spike-timing-dependent plasticity. *J Neurosci* **28**, 2435-2446.

Piomelli D, Astarita G & Rapaka R (2007). A neuroscientist's guide to lipidomics. *Nat Rev Neurosci* **8**, 743-754.

Puente N, Cui Y, Lassalle O, Lafourcade M, Georges F, Venance L, Grandes P & Manzoni OJ (2011). Polymodal activation of the endocannabinoid system in the extended amygdala. *Nat Neurosci* **14**, 1542-1547.

Quilodran R, Rothé M & Procyk E (2008). Behavioral shifts and action valuation in the anterior cingulate cortex. *Neuron* **57**, 314-325.

Rebecchi MJ & Pentyala SN (2000). Structure, function, and control of phosphoinositide-specific phospholipase C. *Physiol Rev* **80**, 1291-1335.

Redgrave P & Gurney K (2006) The short-latency dopamine signal: a role in discovering novel actions? *Nat Rev Neurosci* **7**, 967–975.

Remy S & Spruston N (2007). Dendritic spikes induce single-burst long-term potentiation. *PNAS* **104**, 17192-17197.

Ross RA (2003). Anandamide and vanilloid TRPV1 receptors. *Br J Pharmaco* **140**, 790-801.

Shen W, Flajolet M, Greengard P & Surmeier DJ (2008). Dichotomous dopaminergic control of striatal synaptic plasticity. *Science* **321**, 848-851.

Schultz W, Tremblay L & Hollerman JR (2003). Changes in behavior-related neuronal activity in the striatum during learning. *Trends Neurosci* **26**, 321-328.

Schultz W (2007) Multiple dopamine functions at different time courses. *Annu Rev Neurosci* **30,** 259–288.

Shouval HZ, Bear MF & Cooper LN (2002). A unified model of NMDA receptor-dependent bidirectional synaptic plasticity. *Proc. Natl. Acad. Sci. U. S. A.* **99,** 10831–6.

Sjöström PJ, Rancz EA, Roth A & Häusser M (2008). Dendritic excitability and synaptic plasticity. *Physiol Rev* **88**, 769-840.

Starowicz K, Nigam S & Di Marzo V (2007). Biochemistry and pharmacology of endovanilloids. *Pharmacol Ther* **114**, 13-33.

Tanimura A, Yamazakim M, Hashimotodani Y, Uchigashima M, Kawata S, Abe M, Kita Y, Hashimoto K, Shimizu T, Watanabe M, Sakimura K & Kano M (2010). The Endocannabinoid 2-arachidonoylglycerol produced by diacylglycerol lipase α mediates retrograde suppression of synaptic transmission. *Neuron* **65**, 320-327.

Testa CM, Standaert DG, Young AB & Penney JB Jr (1994). Metabotropic glutamate receptor mRNA expression in the basal ganglia of the rat. *J Neurosci* **14**, 3005-3018.

Tse D, Langston RF, Bethus I, Wood ER, Witter MP & Morris RG (2007). Schemas and memory consolidation. *Science* **316**, 76-82.

Uchigashima M, Narushima M, Fukaya M, Katona I, Kano M & Watanabe M (2007). Subcellular arrangement of molecules for 2-arachidonoyl-glycerol-mediated retrograde signaling and its physiological contribution to synaptic modulation in the striatum. *J Neurosci* **27**, 3663-3676.

Xu JY, Zhang J & Chen C (2012). Long-lasting potentiation of hippocampal synaptic transmission by direct cortical input is mediated via endocannabinoids. *J Physiol* **590**, 2305-2315.

Yamasaki M, Matsui M & Watanabe M (2010). Preferential localization of muscarinic M1 receptor on dendritic shaft and spine of cortical pyramidal cells and its anatomical evidence for volume transmission. *J Neurosci* **30**, 4408-4418.

Yin HH & Knowlton BJ (2006) The role of the basal ganglia in habit formation. *Nat Rev Neurosci* **7,** 464–476.

Yin HH, Mulcare SP, Hilário MR, Clouse E, Holloway T, Davis MI, Hansson AC, Lovinger DM & Costa RM (2009). Dynamic reorganization of striatal circuits during the acquisition and consolidation of a skill. *Nat Neurosci* **12**, 333-341.

Zhu PJ & Lovinger D (2007). Persistent synaptic activity produces long-lasting enhancement of endocannabinoid modulation and alters long-term synaptic plasticity. *J Neurophysiol* **97**, 4386-4389.

ADDITIONAL INFORMATION SECTION

Competing interests:

The authors declare that they have no competing financial interest and conflict of interest.

Author contribution:

Conception and design of the experiments: Y.C., H.B. and L.V.; Y.C., V.P., H. X. and E.F. performed electrophysiological experiments and analysis; H.B., B.D. and S.G. contributed to analytic tools; Y.C., H.B. and L.V. wrote the manuscript and all authors have edited and corrected the manuscript.

Funding:

This work has been supported by grants from INSERM, INRIA, Collège de France, the Agence Nationale pour la Recherche and the Ecole des Neurosciences de Paris.

Acknowledgments:

We thank O Manzoni, S Hormuzdi, P Faure, for helpful suggestions and critical comments; We thank C Ledent (ULB, Belgium) and Denis Hervé (Institut du fer a Moulin, France) for kindly providing $CB_1R^{-/-}$ and D_1R-eGFP mice, respectively.

TABLE

Table 1: Effects of bath-applied drugs on corticostriatal EPSC baseline amplitude.

Bath-applied drugs	Normalized EPSC $_{(baseline-drugs/Baseline-control)}$ amplitude	n, p *
D-AP5 (50µM)	98±4%	n=6, p=0.6076
AM251 (3 µM)	99±5%	n=8, p=0.7988
MCPG (500µM)	94±6%	n=5, p=0.4029
MPEP (10µM)	100±4%	n=4, p=0.9243
Pirenzepine (1µM)	92±7%	n=6, p=0.3739
Nimodipine (1µM)	96±4%	n=4, p=0.3790
Capsazepine (10µM)	100±4%	n=5, p=0.9778
AMG9810 (1µM)	97±8%	n=5, p=0.6800
Picrotoxine (50µM)	96±3%	n=6, p=0.1493
SCH23390 (4µM) + sulpiride (10µM)	102±2%	n=7, p=0.4468

*: None of the bath-applied drugs had a significant effect on baseline. In any cases, only baselines with the bath-applied drugs were compared to EPSC measured after 60 minutes recordings.

FIGURE LEGENDS

Figure 1. A low number of paired stimulations induces spike-timing dependent potentiation.

(A) Scheme of the recording and stimulating sites in corticostriatal slices. Characteristic voltage responses of a MSN to a series of 500 ms current pulses from -150 to +180 pA with current steps increasing by 30 pA (black traces) and to +60 pA above spike threshold (grey trace). (B) STDP protocol: a spike evoked in striatal neuron was paired with cortical stimulation N times at 1Hz. Δt indicates the time delay between pre- and postsynaptic stimulations. $-30<\Delta t<0$ ms and $0<\Delta t<+30$ ms refers to post-pre and pre-post pairings, respectively. (C) 100 post-pre and pre-post pairings (n=10 and 7) induced bidirectional plasticity, *i. e.* tLTP and tLTD, respectively. (D) 75 post-pre and pre-post pairings (n=8 and 6) induced tLTP and tLTD, respectively. (E) 50 post-pre and pre-post pairings (n=7 and 7) induced unidirectional plasticity, *i. e.* no plasticity and tLTD, respectively. (F) 25 post-pre and pre-post pairings (n=11 and 8) did not induce significant plasticity. (G) 10 post-pre and pre-post pairings (n=27 and 9) induced unidirectional plasticity, *i. e.* tLTP and no plasticity, respectively. (H) 5 post-pre and pre-post pairings (n= 16 and 6) induced tLTP and no plasticity, respectively. (I) Summary graph showing the effect of different numbers of pairings (from 100 to 2) on long-term plasticity induction. There is an absence of corticostriatal tLTP with 50, 25 or 2 post-pre pairings while 75-100 or 5-10 post-pre pairings induced significant tLTP. Bidirectional (tLTD and tLTP) STDP is observed for 75-100 pairings, unidirectional (tLTD) STDP for 50 pairings and unidirectional (tLTP) STDP for 5-10 pairings.

Representative traces are the average of 15 EPSCs during baseline (black traces) and 50 min after STDP protocol (grey traces). Error bars represent SD. *: $p<0.05$. ns: not significant.

Figure 2. 10 pairings-tLTP is NMDAR-independent.

(A and B) tLTD induced with 100 (A) or 50 (B) pre-post pairings is CB_1R-mediated. 100 and 50 pre-post pairings induced a potent tLTD (n=7 and 7), which was prevented by AM251 treatment (3μM, n=5 and 7). (C) tLTP induced with 10 post-pre pairings was not prevented by D-AP5 (50μM, n=13), indicating that this tLTP was not NMDAR-mediated. Summary bar graphs illustrating that 100 post-pre pairing tLTP is NMDAR-mediated since it is prevented by D-AP5 treatment, while 10 post-pre pairings tLTP is NMDAR-independent.

Representative traces are the average of 15 EPSCs during baseline (black traces) and 50 min after STDP protocol (grey traces). Error bars represent SD.

Figure 3. 10 pairings-tLTP induction involves postsynaptic 2-AG signaling.

(A and B) Summary graphs of pharmacological experiments delineating the intracellular signaling pathways involved in 10 pairings-induced tLTP. (A) tLTP was prevented by inhibition of group-I mGluR with MCPG (500μM, n=5) or of DAGLα by i-THL (10μM, n=5). (B) Summary bar graphs showing that LTP was mGluR5- and M_1R-mediated. Indeed, tLTP was prevented by inhibition of group-I mGluR with MCPG (500μM, n=5) and more spefically of mGluR5 with MPEP (10μM, n=6); inhibition of M_1R also prevented tLTP (1μM pirenzepine, n=6). Downstream these receptors, inhibition of postsynaptic G-protein coupled receptors (with i-GDP-β-S 2mM, n=10), PLCβ (with 5mM i-U73122, n=5), DAGLα (with 10μM i-THL, n=5), show the involvement of the PLCβ and 2-AG synthesis. In addition, bar graphs show the involvement of postsynaptic intracellular calcium (10mM i-BAPTA, n=5) and VSCCs (1μM nimodipine, n=5), since their blockade prevented the expression of tLTP. (C) Repeated brief application of 2-AG induces LTD. A serie of 100 2-AG puffs (100μM, 300 ms duration each) delivered at 1Hz at the vicinity (50-100μm) of the recorded striatal neuron, induced LTD in the absence of any STDP protocol (n=8). This 2-AG-mediated LTD

was prevented by AM251 (3μM, n=6). (D) Limited brief application of 2-AG induces LTP. Application of 10 2-AG puffs (100μM, 300 ms duration each) delivered at 1Hz were able to induce LTP in the absence of any STDP paired stimulation (n=8). Inhibition of CB_1R with bath-applied AM251 (3μM, n=5) prevented the induction of LTP by 2-AG puffs.

The prefix "i" indicates that the drug was applied in the recorded postsynaptic neuron through the patch-clamp pipette. Representative traces are the average of 15 EPSCs during baseline (black traces) and 50 min after STDP protocol (grey traces). Error bars represent SD.

Figure 4. 10 pairings-tLTP is CB_1R-mediated.

(A) 10 pairings-tLTP is prevented by a specific CB_1R inhibitor, AM251 (3μM, n=6). (B) 10 post-pre pairings induced tLTP in wild-type $CB_1R^{+/+}$ mice (n=10) while no plasticity was observed in $CB_1R^{-/-}$ mice (n=16). (C) Summary bar graphs with $CB_1R^{-/-}$ and $CB_1R^{+/+}$ mice illustrate that eCB-tLTP is CB_1R-mediated both in juvenile $P_{(18-25)}$ and adult $P_{(60-90)}$ animals.

Representative traces are the average of 15 EPSCs during baseline (black traces) and 50 min after STDP protocol (grey traces). Error bars represent SD. *: $p<0.05$. ns: not significant.

Figure 5. eCB-LTP is also TRPV1-mediated

(A) 10 pairings-tLTP was prevented when TRPV1 was inhibited by capsazepine (10μM, n=6). (B) Summary bar graphs show that capsazepine (10μM, n=6) or AMG9810 (1μM, n=5) prevented the 10 pairings tLTP.

Representative traces are the average of 15 EPSCs during baseline (black traces) and 50 min after STDP protocol (grey traces). Error bars represent SD. *: $p<0.05$. ns: non-significant.

Figure 6. eCB-tLTP is induced in both striatopallidal and striatonigral MSNs and is dopamine-dependent

(A) 15 pairings-tLTP is observed in both striato-pallidal (D1-eGFP positive neurons, $D1^+$, n=7) and striato-nigral (D1-eGFP negative neurons, non-$D1^+$, n=9) MSNs. (B) Co-application of antagonists of D_1R and D_2R, SCH23390 (4µM) and sulpiride (10µM), prevents eCB-tLTP (n=7). (C) tLTP was induced in presence of the D_1R antagonist, SCH23390 (4µM, n=7) while no plasticity was observed with the D_2R antagonist, sulpiride (10µM, n=6).

Representative traces are the average of 15 EPSCs during baseline (black traces) and 40 (A) and 50 (B and C) min after STDP protocol (grey traces). Error bars represent SD. *: $p<0.05$. ns: non-significant.

Figure 7. Corticostriatal eCB-tLTP is homosynaptic

(A) Scheme and raw traces illustrating paired recordings of MSNs (perisomatic distance<50µm): one neuron received a 10 pairing STDP protocol (pre- and postsynaptic stimulations) while the other one only received 10 presynaptic stimulations. tLTP was induced exclusively in the neuron with the STDP protocol (10 post-pre pairings, black circles, n=6) while no significant plasticity was observed in the neighboring neuron (presynaptic stimulations only, n=6). These results indicate a homosynaptic characteristic of eCB-tLTP. (B) Inhibition of the $GABA_A$ transmission with picrotoxin did not affect eCB-tLTP magnitude but controls the time-dependence of eCB-tLTP. With bath-applied picrotoxin (50µM), a potent tLTP was induced by 10 pre-post pairings (n=6; blue) while no significant plasticity was observed with 10 post-pairings (n=7; black). The occurrence and magnitude of tLTP were not affected by a blockade of $GABA_A$ transmission since induced plasticities were not significantly different from the ones observed in control conditions. This tLTP induced with 10 pre-post pairings under $GABA_A$ receptors blockade is eCB-mediated since prevented with bath-application of AM251 (3µM). GABAergic microcircuits are not involved in the synaptic efficacy changes themselves but control the time-dependence of the eCB-tLTP.

Representative traces are the average of 15 EPSCs during baseline (black traces) and 50 min after STDP protocol (grey traces). Error bars represent SD. *: $p<0.05$. ns: not significant.

Figure 8. Bidirectional eCB synaptic plasticity in a single neuron

(A and B) eCB-tLTP and eCB-tLTD can be induced sequentially in the same neuron. Representative experiments illustrating in (A) an eCB-tLTP event (induced by 10 post-pre pairings, red vertical line) followed by an eCB-tLTD occurrence (induced by 50 pre-post pairings, blue vertical line) and in (B) the reversed sequence (eCB-tLTD followed by eCB-tLTP). In both cases, the neurons come back to baseline level after the full sequence.

Single EPSC amplitudes (empty grey circles) and averaged data (empty white circles) are represented.

Figure 1

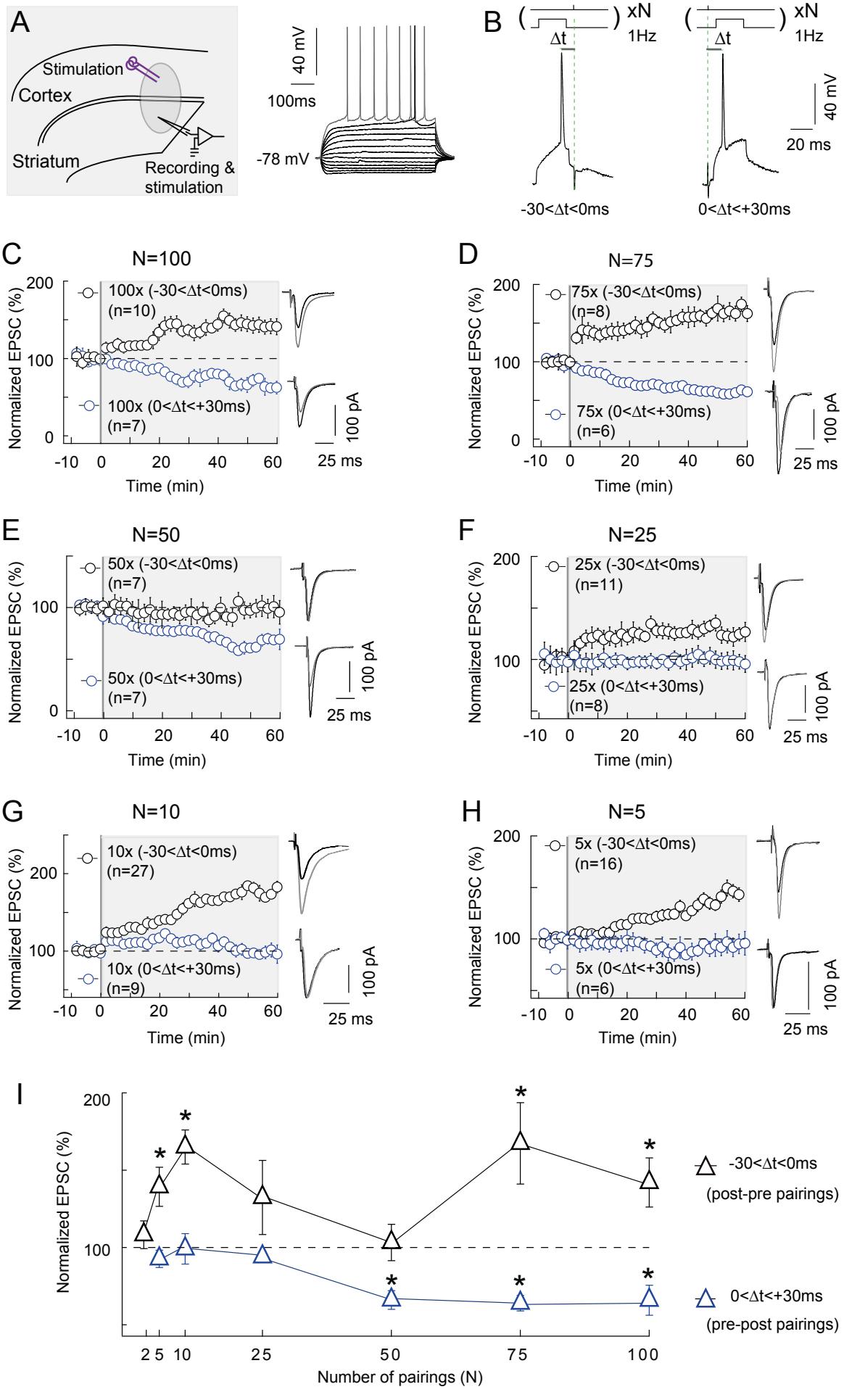
A
Stimulation
Cortex
Striatum
Recording &
stimulation
40 mV
100ms
-78 mV
B
Δt
xN
1Hz
40 mV
20 ms
-30<Δt<0ms
0<Δt<+30ms
C
N=100
100x (-30<Δt<0ms)
(n=10)
100x (0<Δt<+30ms)
(n=7)
Normalized EPSC (%)
Time (min)
100 pA
25 ms
D
N=75
75x (-30<Δt<0ms)
(n=8)
75x (0<Δt<+30ms)
(n=6)
E
N=50
50x (-30<Δt<0ms)
(n=7)
50x (0<Δt<+30ms)
(n=7)
F
N=25
25x (-30<Δt<0ms)
(n=11)
25x (0<Δt<+30ms)
(n=8)
G
N=10
10x (-30<Δt<0ms)
(n=27)
10x (0<Δt<+30ms)
(n=9)
H
N=5
5x (-30<Δt<0ms)
(n=16)
5x (0<Δt<+30ms)
(n=6)
I
Normalized EPSC (%)
Number of pairings (N)
-30<Δt<0ms
(post-pre pairings)
0<Δt<+30ms
(pre-post pairings)

Figure 2

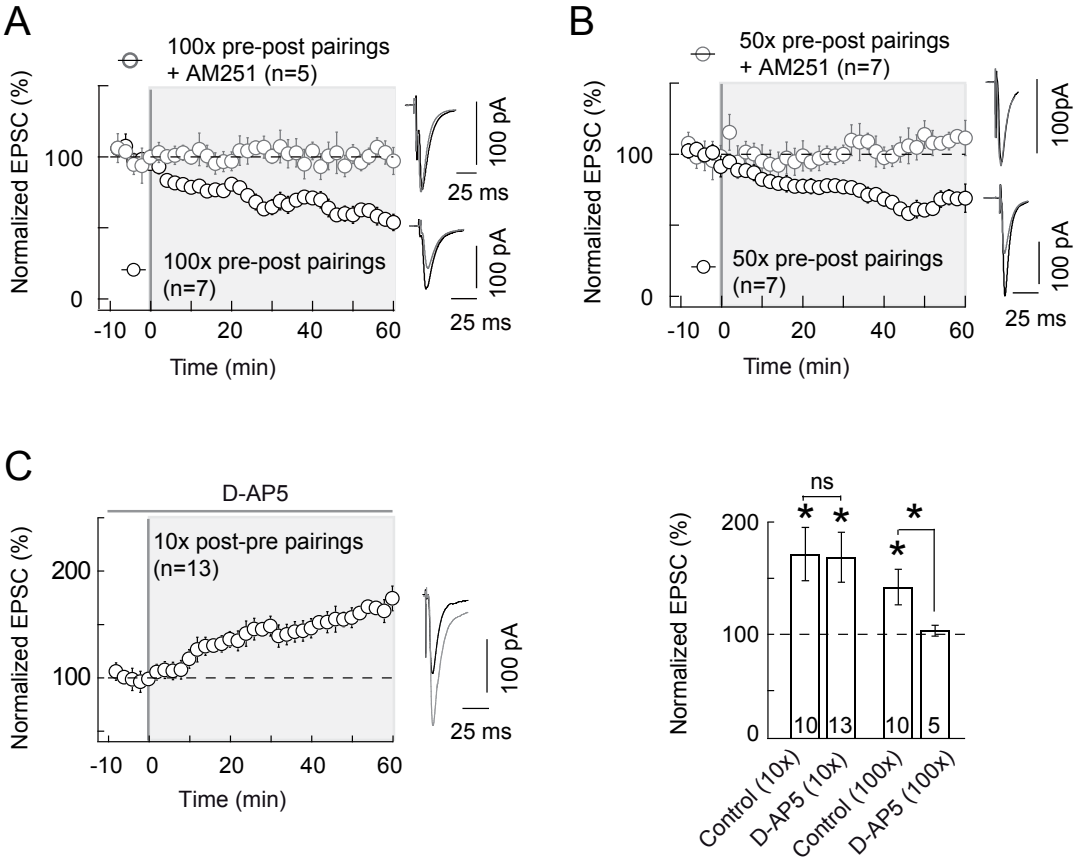
A
100x pre-post pairings
+ AM251 (n=5)
100x pre-post pairings
(n=7)
Normalized EPSC (%)
100
0
-10 0 20 40 60
Time (min)
100 pA
25 ms
100 pA
25 ms
B
50x pre-post pairings
+ AM251 (n=7)
50x pre-post pairings
(n=7)
Normalized EPSC (%)
100
0
-10 0 20 40 60
Time (min)
100pA
100 pA
25 ms
C
D-AP5
10x post-pre pairings
(n=13)
Normalized EPSC (%)
200
100
-10 0 20 40 60
Time (min)
100 pA
25 ms
ns
*
*
*
*
Normalized EPSC (%)
200
100
0
10
13
10
5
Control (10x)
D-AP5 (10x)
Control (100x)
D-AP5 (100x)

Figure 3

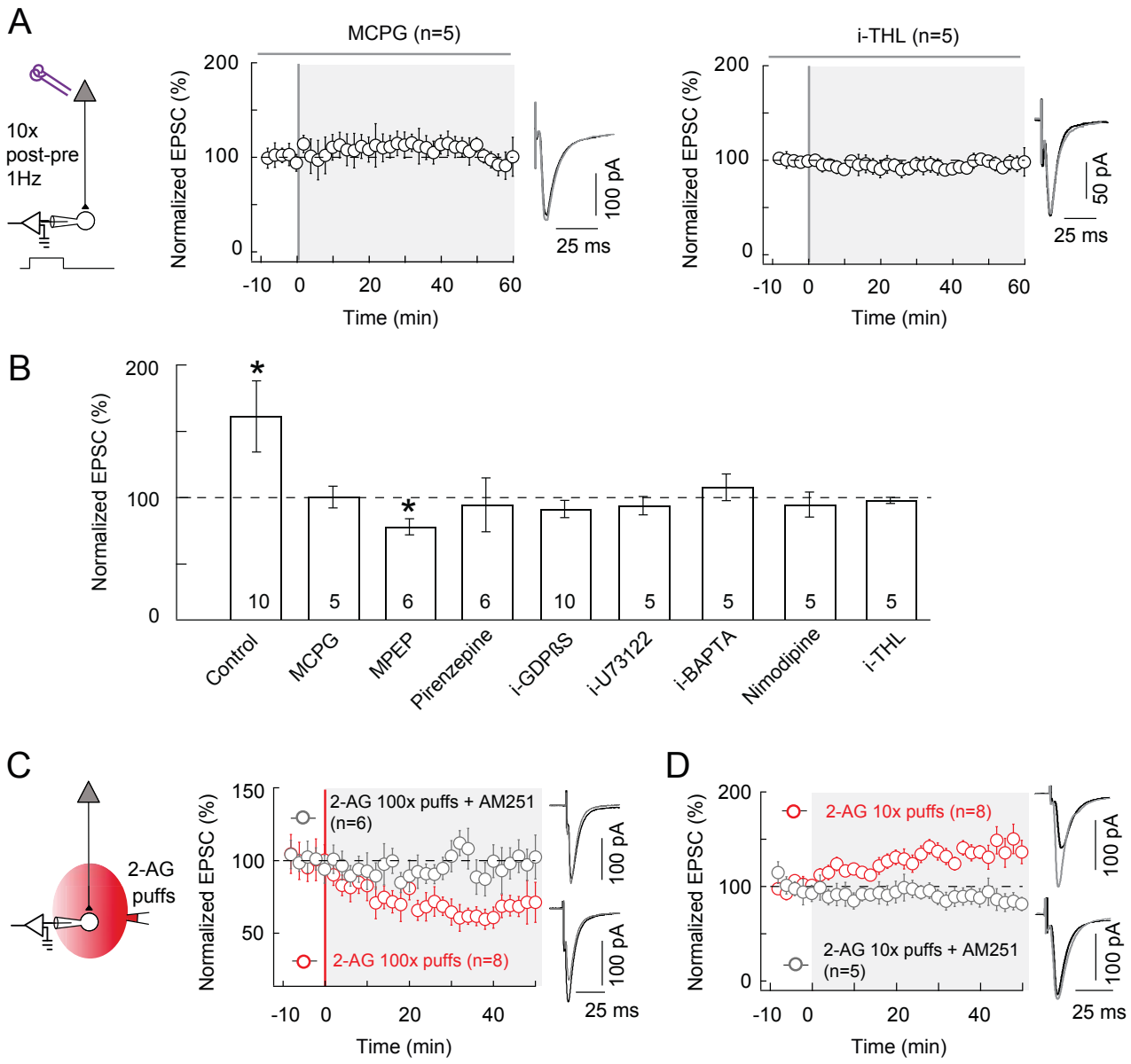
A
10x
post-pre
1Hz
MCPG (n=5)
Normalized EPSC (%)
200
100
0
-10
0
20
40
60
Time (min)
100 pA
25 ms
i-THL (n=5)
50 pA
B
*
10
5
6
6
10
5
5
5
5
Control
MCPG
MPEP
Pirenzepine
i-GDPβS
i-U73122
i-BAPTA
Nimodipine
i-THL
C
2-AG
puffs
150
50
2-AG 100x puffs + AM251
(n=6)
2-AG 100x puffs (n=8)
D
2-AG 10x puffs (n=8)
2-AG 10x puffs + AM251
(n=5)

Figure 4

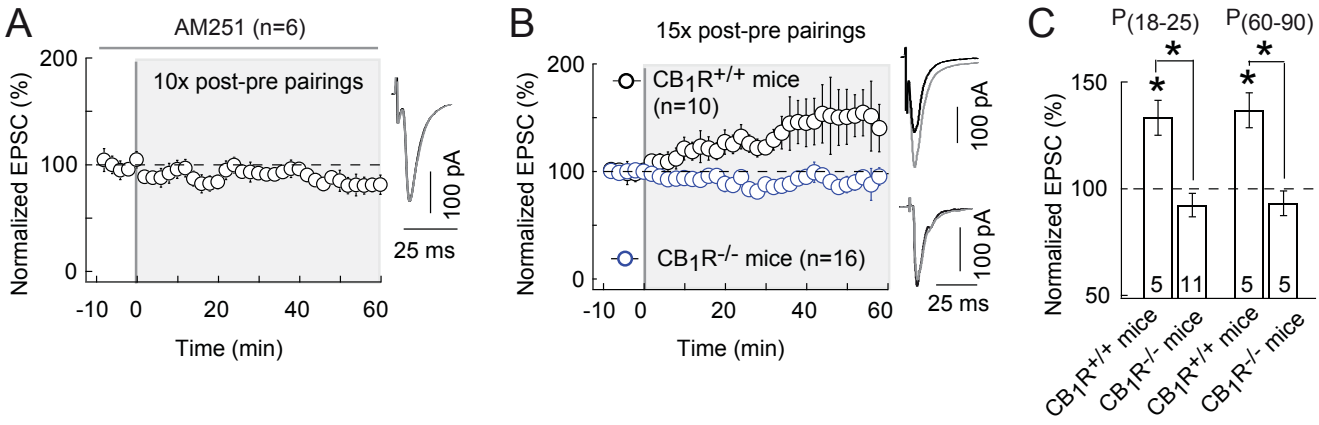
A
AM251 (n=6)
10x post-pre pairings
Normalized EPSC (%)
200
100
0
-10
0
20
40
60
Time (min)
100 pA
25 ms
B
15x post-pre pairings
CB1R+/+ mice
(n=10)
CB1R-/- mice (n=16)
Normalized EPSC (%)
Time (min)
100 pA
25 ms
C
P(18-25)
P(60-90)
Normalized EPSC (%)
150
100
50
5
11
5
5
CB1R+/+ mice
CB1R-/- mice
CB1R+/+ mice
CB1R-/- mice

Figure 5

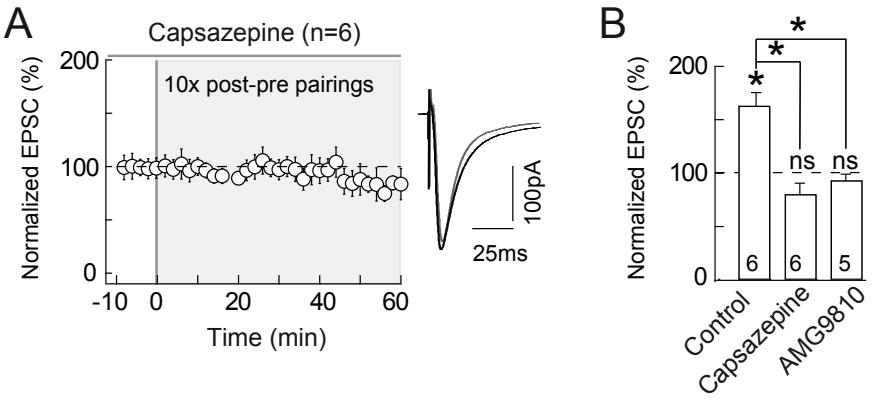
A
Capsazepine (n=6)
10x post-pre pairings
Normalized EPSC (%)
200
100
0
-10
0
20
40
60
Time (min)
100pA
25ms
B
Normalized EPSC (%)
200
100
0
*
*
*
ns
ns
6
6
5
Control
Capsazepine
AMG9810

Figure 6

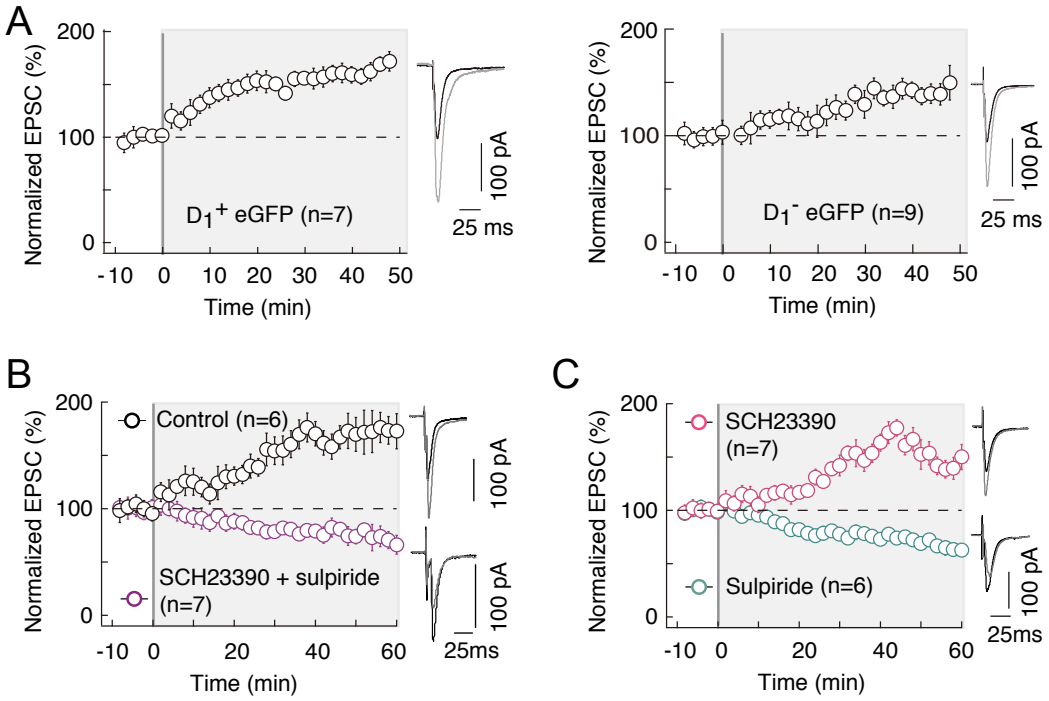
A
Normalized EPSC (%)
200
100
0
-10 0 10 20 30 40 50
Time (min)
D1+ eGFP (n=7)
100 pA
25 ms
D1- eGFP (n=9)
B
Control (n=6)
SCH23390 + sulpiride
(n=7)
25ms
C
SCH23390
(n=7)
Sulpiride (n=6)

Figure 7

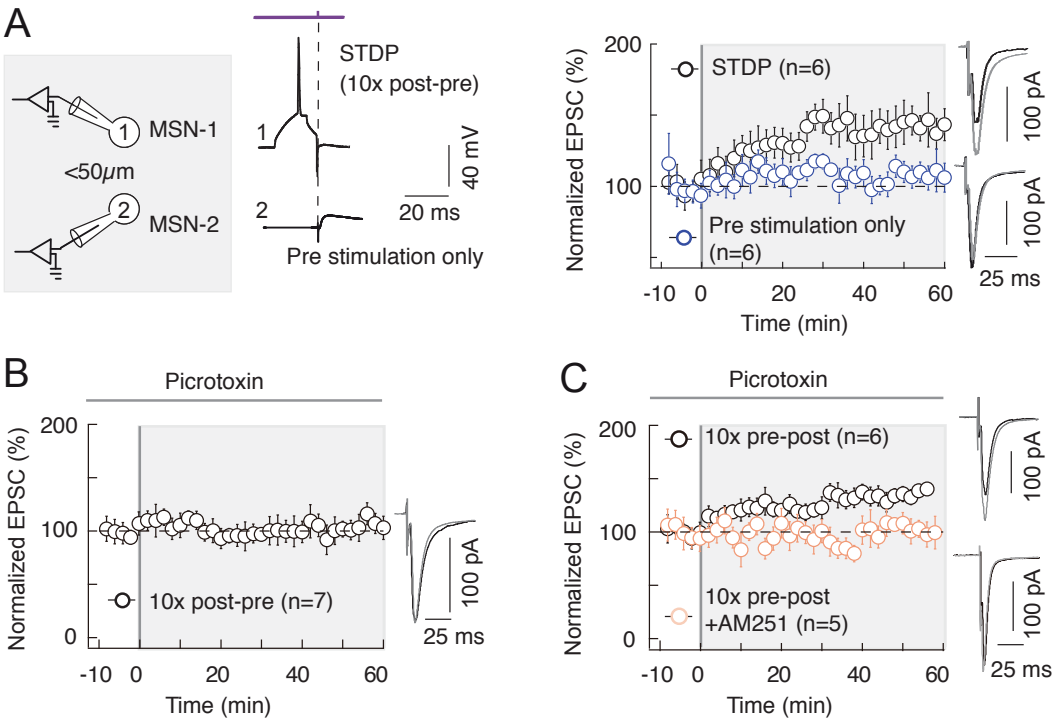
A
MSN-1
<50μm
MSN-2
STDP
(10x post-pre)
40 mV
20 ms
Pre stimulation only
STDP (n=6)
Pre stimulation only
(n=6)
Normalized EPSC (%)
Time (min)
100 pA
25 ms
B
Picrotoxin
10x post-pre (n=7)
C
Picrotoxin
10x pre-post (n=6)
10x pre-post
+AM251 (n=5)

Figure 8

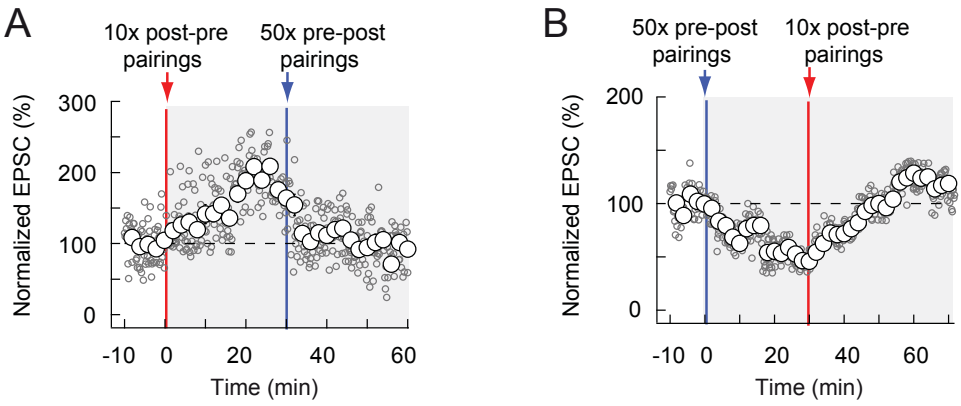
A
10x post-pre pairings
50x pre-post pairings
Normalized EPSC (%)
300
200
100
0
-10
0
20
40
60
Time (min)
B
50x pre-post pairings
10x post-pre pairings
Normalized EPSC (%)
200
100
0
-10
0
20
40
60
Time (min)